

# Simulations for the experiments of Roberts, Chang and McCready

Jie Li, Yuriko Y. Renardy  
Department of Mathematics and ICAM  
Virginia Polytechnic Institute and State University  
Blacksburg, VA 24061-0123, U.S.A.

December 7, 1998

## 1 Introduction

Simulations are performed for two-layer Couette flow with the notation of [2]. The computational domain represents a spatially periodic case with wavelength  $2\pi/\alpha$ . Length is made dimensionless with respect to plate separation, which is 1 cm in the experiments. Interfacial tension is 10 dyn/cm. Two cases are examined. The fluids are density-matched in both cases, so that gravity can be neglected. The fluid parameters for the kinematic viscosities are slightly different for case 1 and case 2. The main difference between the cases is the upper plate speed. Case 1 represents a slower speed where waves are present without fingering, and case 2 is at a higher upper plate speed, with fingering. The data from Randy Roberts are shown in Figure 1 for case 1, and Figure 2 for case 2.

Figure 1: The top denotes the experimental wave tracing and the bottom represents the simulated result.



Figure 2: Sheet formation is shown. the top of the image is the more viscous phase, and the bottom is the less viscous phase. The dimensions are approximately 0.8 cm in the horizontal direction and 0.65 cm in the vertical direction. The regime is not spatially periodic. The sheet-like formations can extend up to about 1-2 cm in length.

According to Randy, the experiments are conducted such that at one plate speed, periodic or non-stationary solitary waves are observed, but as this speed is increased at slow increments, and time is given between each increment, the sheet-like formations begin to form.

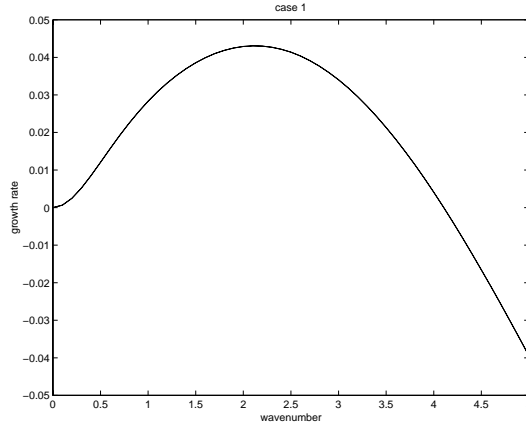


Figure 3: Linear theory for dimensionless growth rate  $\text{Re}\sigma$  vs dimensionless wavenumber  $\alpha$ , notation as in Coward et. al (1997).

## 2 Parameter set 1

The undisturbed interface lies at 0.47cm above the lower plate. The upper plate speed is 29 cm/s. The kinematic viscosities of the lower and upper fluids are  $0.0795 \text{ cm}^2/\text{s}$  and  $5 \text{ cm}^2/\text{s}$ , respectively. The densities of the lower and upper fluids are  $1.113 \text{ g/cm}^3$ . For these fluid parameters, the linear growth rate vs wavenumber is shown in Figure 3. The maximum growth rate mode is at wavenumber 2.1, with  $\sigma = 0.043 - 2i$ , corresponding to a wavelength of 3 cm.

The situation with wavelength 3 cm is simulated until saturation is achieved. We start from a very small perturbation amplitude to keep the flow in the linear regime for a long time. We set  $A(0) = 0.001$ . At the left of Fig. 4, we plot, on a  $\log_{10}$ -linear scale, the evolution of the maximum amplitude  $A(t)$  against the time. Until  $t = 60$ , the numerical and theoretical growth rates agree, the difference between them being 2%, and the agreement zone is over one and a half decade. The evolution of the maximum of the vertical velocity  $V$  (middle of Fig. 4) and  $L_2$  norm (right of Fig. 4) against time are shown also in figure 4 and good agreement is also obtained. This calculation is carried out on a  $256 \times 160$  mesh.

Corresponding to figure 4, the temporal evolution of interface is shown in Figure 5 for time  $t = 50, 80, 100, 150, 180$  and  $200$ . As the interface moves vertically under the viscosity-jump instability, the two fluids do not penetrate into each other in the same manner. Note that the upper fluid is more viscous than the lower one. We observe that at  $t = 100$ , the interface trough is more narrow than interface crest and the interface loses its shape symmetry. At this stage, we can conclude already from mass conservation that the upper fluid penetrate faster into lower fluid. This can be explained by the fact that the low viscosity liquid provides less resistance, making it easier for the high viscosity liquid to penetrate inside it. An analogy is that when inertia is important, a high density fluid penetrates easily into a low density fluid. It is evident from Figures 4 and 5 that the flow saturates to traveling waves. Interface shows almost symmetrical form of crest and trough. The maximum of saturation interface high is about 0.552 (maximum of the interfacial amplitude 0.082).

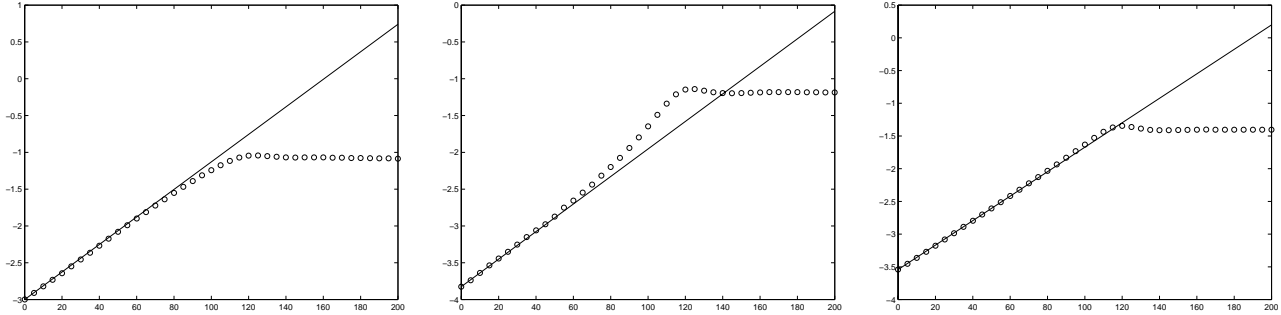


Figure 4:  $\text{Log}_{10}$  plots of the maximum of interface position, the maximum vertical velocity  $V$  and the  $L_2$  norm against time for the flow :  $A(0) = 0.001$ ,  $\alpha = 2.1$ ,  $\text{Re}_1 = 358.3546$ ,  $m = 0.0159$ ,  $l_1 = 0.47$ ,  $T = 0.0630$ , equal densities, and zero gravity. Theoretical linear growth rate for the interfacial mode is 0.0431. Solid lines represents theoretical growth and circles represent the calculation. The calculation is carried out on a  $256 \times 160$  mesh.

### 3 Parameter set 2

The undisturbed interface lies at 0.49cm above the lower plate. The upper plate speed is 49.7 cm/s. The kinematic viscosities of the lower and upper fluids are  $0.085 \text{ cm}^2/\text{s}$  and  $5 \text{ cm}^2/\text{s}$ , respectively. The densities of the lower and upper fluids are  $1.113 \text{ g/cm}^3$ . For these fluid parameters, the linear growth rate vs wavenumber is shown in Figure 6. The maximum growth rate mode is at wavenumber 3.0, with  $\sigma = 0.05 - 2.9i$ , corresponding to a wavelength of 2 cm.

First, the situation with wavelength 2.09 cm (wavenumber 3) is simulated . We set the initial amplitude  $A(0) = 0.05$ . The temporal evolution of interface shape is shown in Figure 7 for  $t = 0, 10, 20, 30, 35$  and 40. The eventual flowfield is qualitatively similar to the previous case. The flow saturates to traveling waves. Interface shows almost symmetrical form of crest and trough.

Secondly, we investigate the situation with wavelength 4 cm (wavenumber 1.57) is simulated. The eventual flowfield is qualitatively different from the previous case in that it is not steady but varies with time. The temporal evolution is shown in Figure 8

It is evident from Figures 8 that the interface shape eventually attains a steep trough. The situation is quite different from the previous case. The interface trough is no longer symmetric, but turns to left direction. We attribute this difference to the reduction of surface tension effect on long wave. Fingering will not occur because the effects of viscosity difference, interfacial tension and speed are such that the wave does not deform sufficiently horizontally to induce fingering. The situation when the upper plate speed is increased gradually to the prescribed value is also investigated. We increase the speed linearly during a time  $\Delta T$ .  $\Delta T = 20, 50, 100$ , and 200 have been investigated. There are no significant difference in the final interface shape among these situations. Interface evolution for  $\Delta T = 20$  case is shown in Figure 9 for time  $t = 10, 20, 25, 30, 35, 40, 90$  and 100. The interface evolution history is different from the precedent case, but the final interface is still similar.

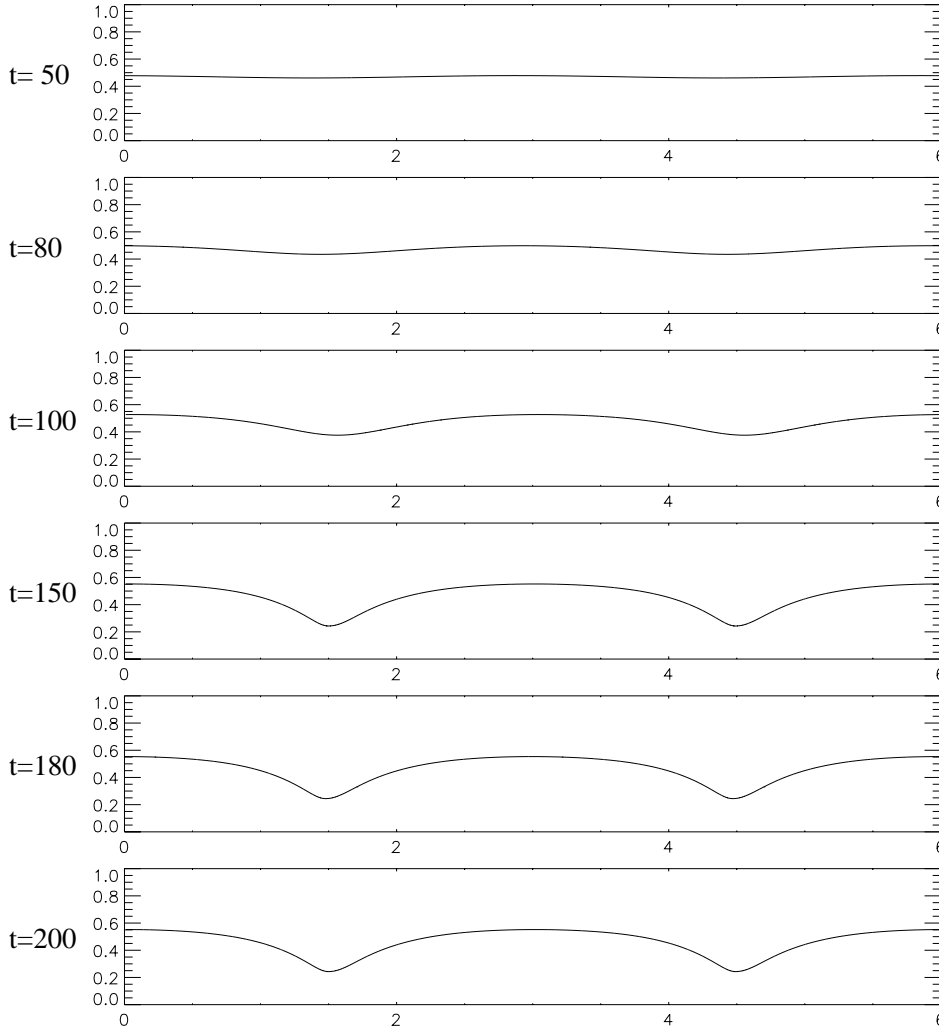


Figure 5:  $Re_1 = 358.3546$ ,  $m = 0.0159$ ,  $l_1 = 0.47$ ,  $T = 0.0630$ . Spatial period 3cm. Temporal evolution of interface shape at times  $t= 50, 80, 100, 150, 180$  and  $200$ .

## 4 Other wavenumbers

In the precedent section, we have seen that for the long wave (wave length = 4 cm), the interface trough loses its symmetrical form and the higher viscosity fluid (upper fluid) penetrates more into the lower viscosity fluid (bottom fluid). We distribute this change to the reduction of surface tension effect for long wave. In this section, we investigate the situation with wavelength = 10 cm and 20 cm. The corresponding wavenumbers are 0.628 and 0.314. We show here the case wavelength = 10 cm. The initial amplitude  $A(0) = 0.01$ . The interface evolution is shown in Fig. 10 for time  $t = 30, 50, 100, 200, 300, 350$  and  $400$ . At  $t = 30$ , interface shows one wavelength 10 and we observe only one trough. But the wave with wavelength = 10 is a very weak mode and is perturbed by most fast mode. At time  $t = 50$ , we see the first trough continues to steep. At meantime, a another trough begins to appear near the first trough. At time  $t = 100$ , the second trough is now evident. As the

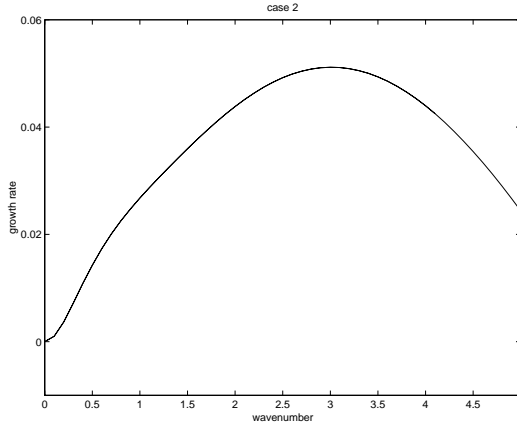


Figure 6: Linear theory for dimensionless growth rate  $Re\sigma$  vs dimensionless wavenumber  $\alpha$ , notation as in Coward et. al (1997).

flow evolves ( $t = 200, 300, 350$  and  $400$ ), the two troughs increase and the distance between them increases also. They are expected to equally distributed at the end. Therefore we only observed the wave mode with half initial wavelength.

## 5 Influence of surface tension

The influence of surface tension on the atomization is investigated. We use all the parameters of set 2 but with a small surface tension parameter  $T$ . In the set 2,  $T$  is equal to 0.037 and we use here a  $T$  equal to 0.001. The initial wavelength is 4 cm (wavenumber 1.57) with the disturbance amplitude 0.05. The temporal evolution is shown in Figure 11. Compared to Figure 8, all the parameters are the same but the surface tension parameter  $T$  is small. In the early period, the interface is still flat and the surface tension effect is less important, the wave shape observed here (for time  $T = 15$ ) is quite similar to the case shown in Figure 8. However, when the flow evolves more and more into nonlinear regime, the upper fluid penetrates into the lower fluid and forms a finger (for time  $T = 20$ ). The surface tension plays now a important role in the determination of flow behavior. In Figure 11, the retraction force caused by the surface tension is small in comparison with Figure 11 and the finger of the upper fluid continues to be stretched by the flow (time  $T = 25, 27$  and  $28$ ) and breaks-up, producing a series of droplets of the upper fluid.

## 6 High Reynolds number

We have also investigated the high Reynolds number flow. In the experiment 2, if we double the upper plate speed, the Reynolds number will be 1149. We simulate this flow with wavelength 3 cm whose initial amplitude is 0.01. The temporal evolution is shown in Figure 12. The behavior of the flow until time  $T = 80$  is very similar to Figure 8 and we see the formation of a finger of upper fluid. However, wavelength 3 cm is too long for this

Reynolds. We see for  $T = 80$  another wave with shorter wavelength, This short wave travels with different speed and its amplitude increases as the time evolves. At time  $T = 80$ , this wave is very small and its trough locates behind the former finger. At  $T = 100$ , it travels to place before the former finger. At  $T = 140$ , it is again behind the finger and at this time we see clearly another small finger. Finally, the two fingers will equally distributed in space (time  $T = 200$ ).

## **Acknowledgement**

This research was sponsored by the National Science Foundation under Grants No. CTS-9612308.

## References

- [1] R. M. Roberts, H. -C. Chang and M. J. McCready, Mechanism of atomization in a two-layer Couette flow, NASA Microgravity Conference 1998.
- [2] A. V. Coward, Yuriko Renardy, M. Renardy, J. R. Richards, Temporal evolution of periodic disturbances in two-layer Couette flow, *J. Comp. Phys.* **132** (1997) 346-361.

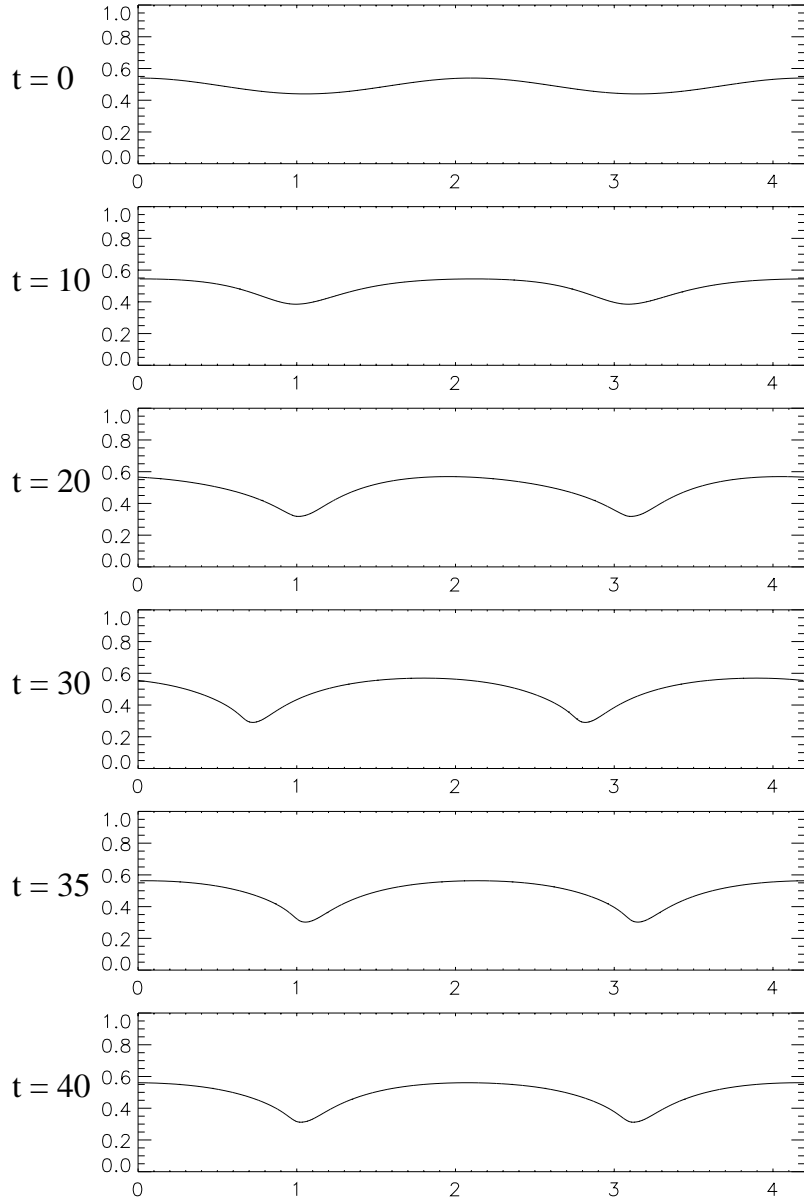


Figure 7:  $Re = 574.54$ ,  $m = 0.017$ ,  $l_1 = 0.49$ ,  $T = 0.037$ . Spatial period 2.09 cm. Temporal evolution of interface shape at times  $t = 0, 10, 20, 30, 35$  and  $40$ .

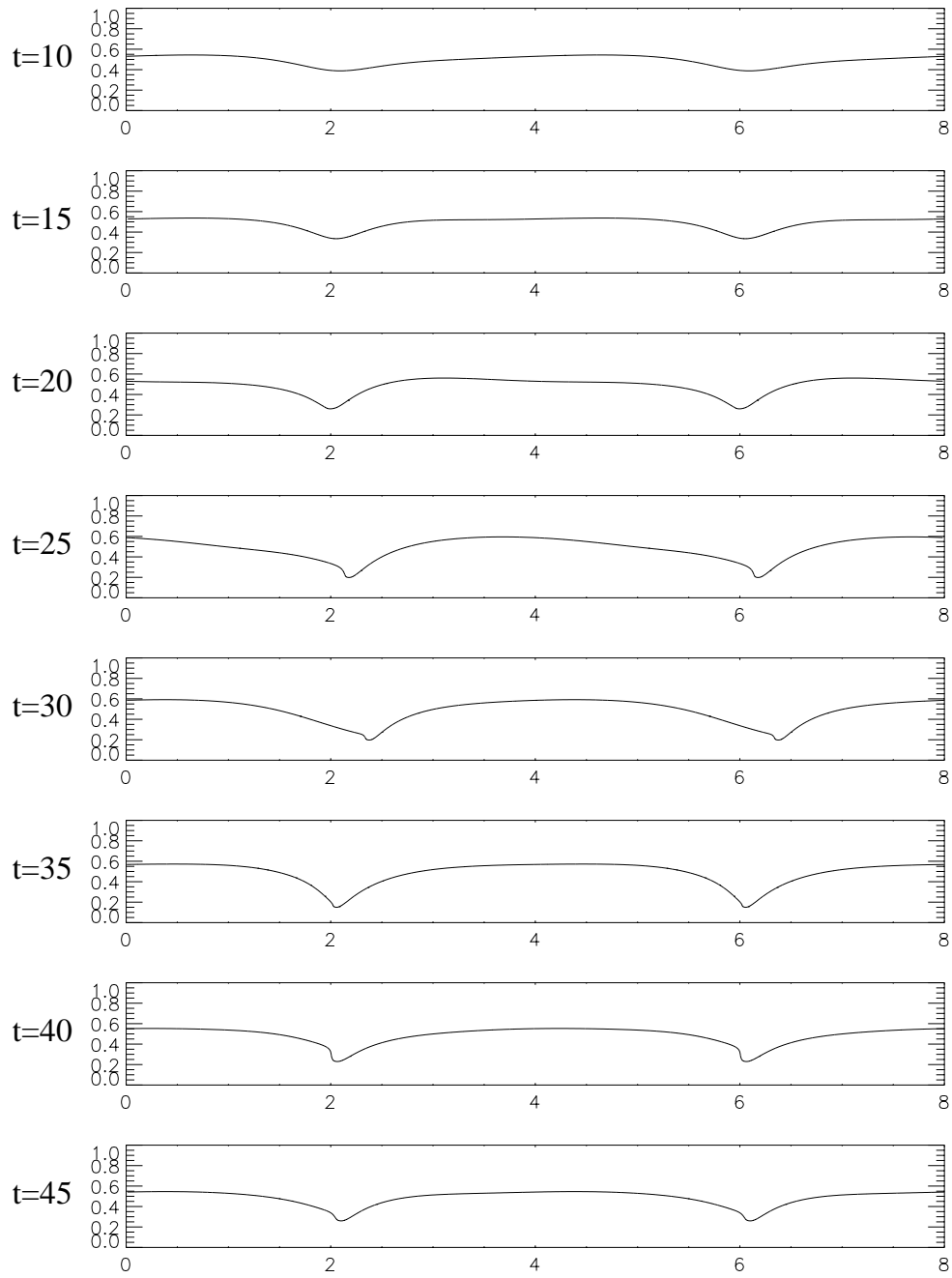


Figure 8:  $Re = 574.54$ ,  $m = 0.017$ ,  $l_1 = 0.49$ ,  $T = 0.037$ . Spatial period 4cm. Temporal evolution of interface shape at times  $t= 10, 15, 20, 25, 30, 35, 40$  and  $45$ .

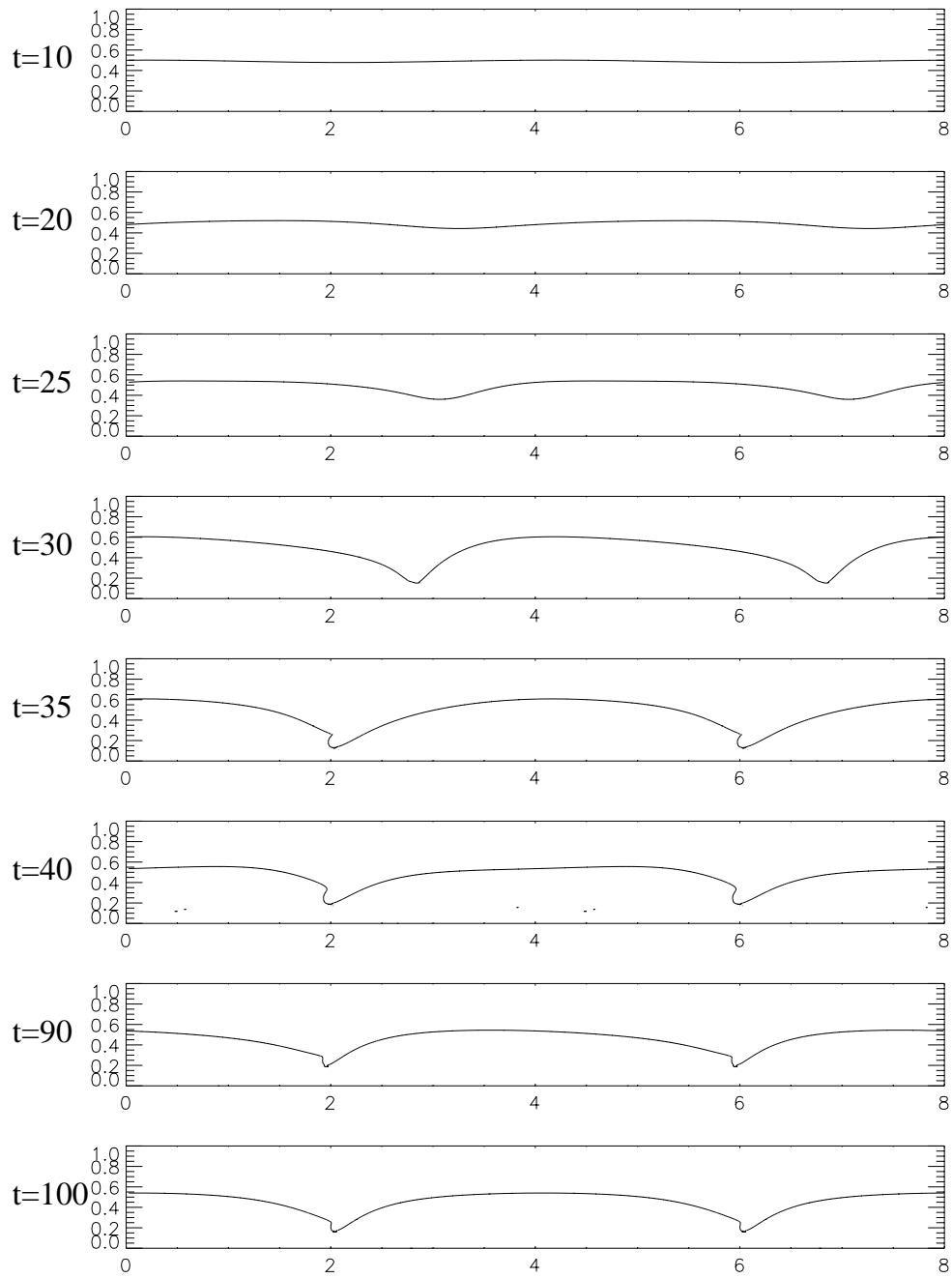


Figure 9:  $Re = 574.54$ ,  $m = 0.017$ ,  $l_1 = 0.49$ ,  $T = 0.037$ . Spatial period 4cm. Temporal evolution of interface shape at times  $t= 10, 20, 25, 30, 35, 40, 90$  and  $100$ . The upper plate speed increases linearly from zero to  $49.7$  cm/s during a time 20 second.

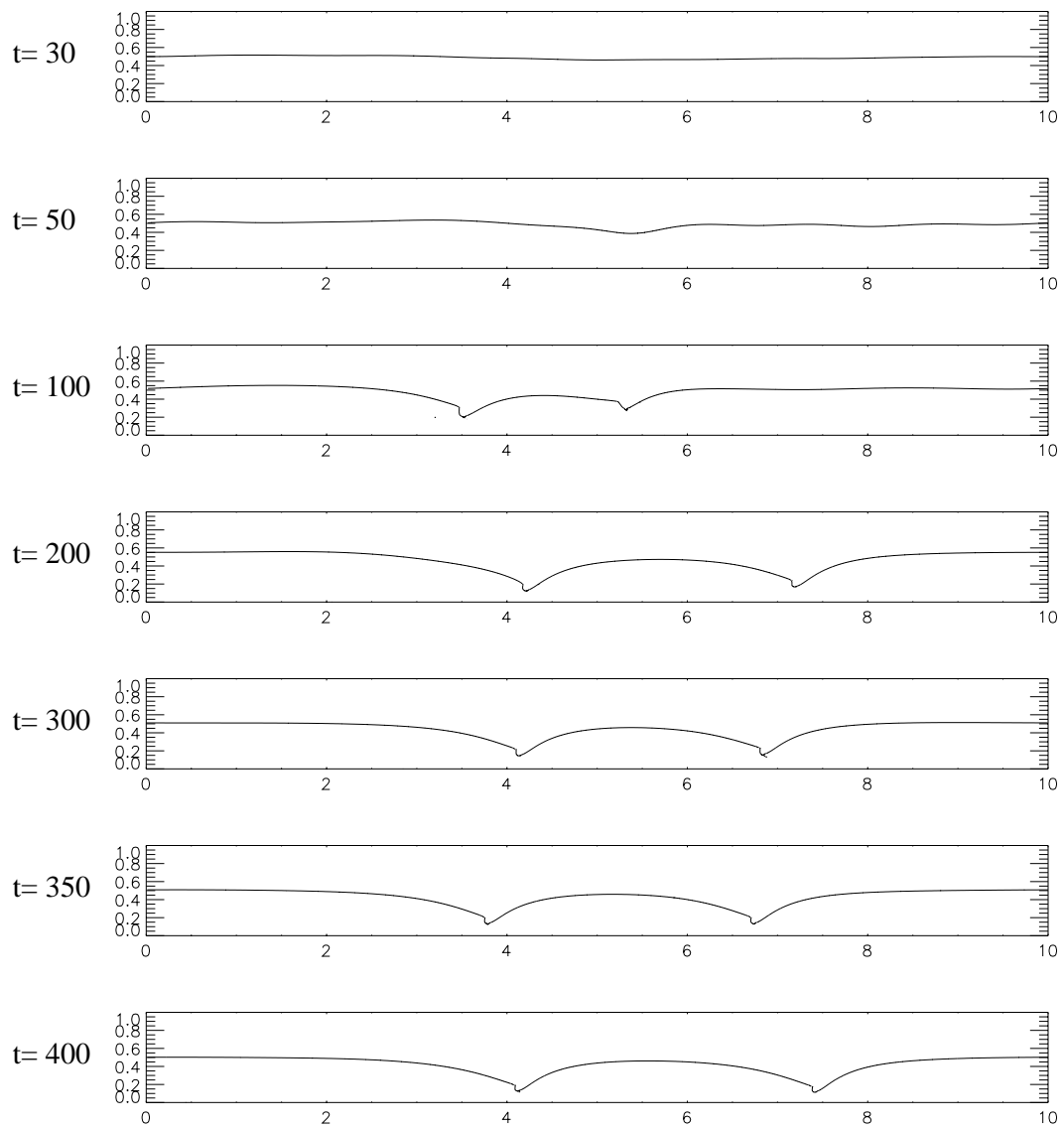


Figure 10:  $Re = 574.54$ ,  $m = 0.017$ ,  $l_1 = 0.49$ ,  $T = 0.037$ . Spatial period 4cm. Temporal evolution of interface shape at times  $t= 50, 100, 200, 300, 350$  and  $400$ .

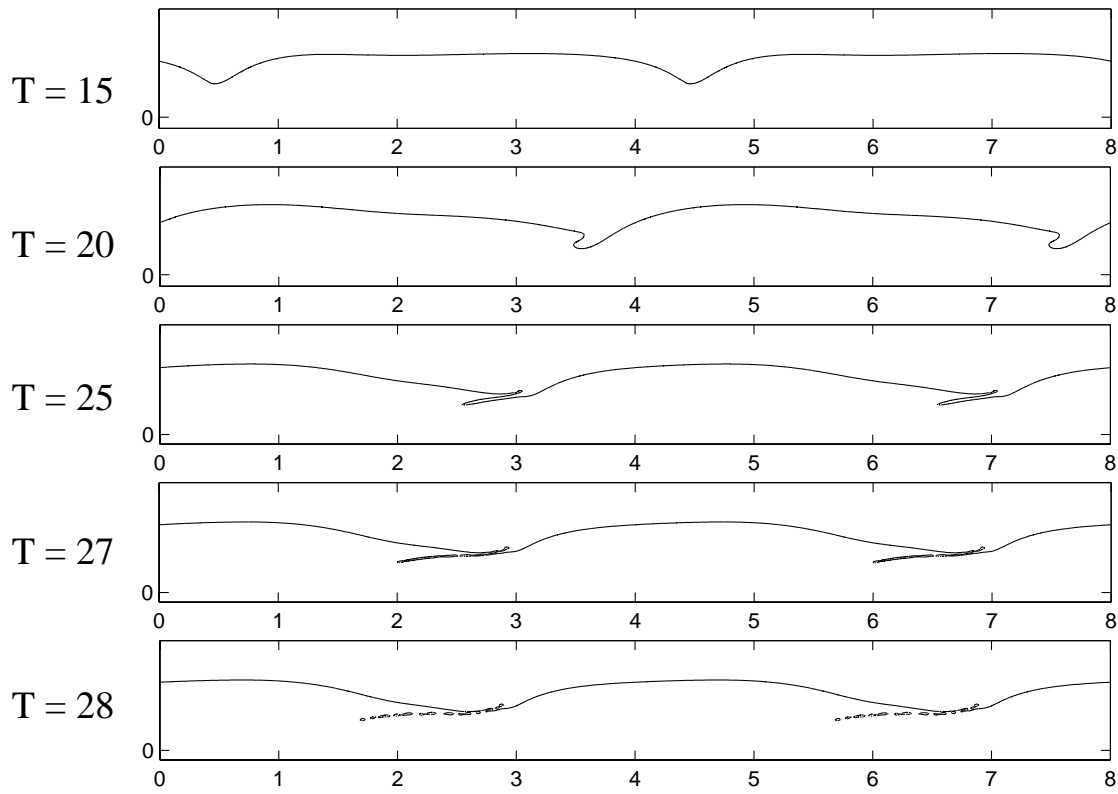


Figure 11: Reduction effect of surface tension :  $T = 0.001$ .  $Re = 574.54$ ,  $m = 0.017$ ,  $l_1 = 0.49$ . Spatial period 4cm. Temporal evolution of interface shape at times  $t = 15, 20, 25, 27$  and  $28$ .

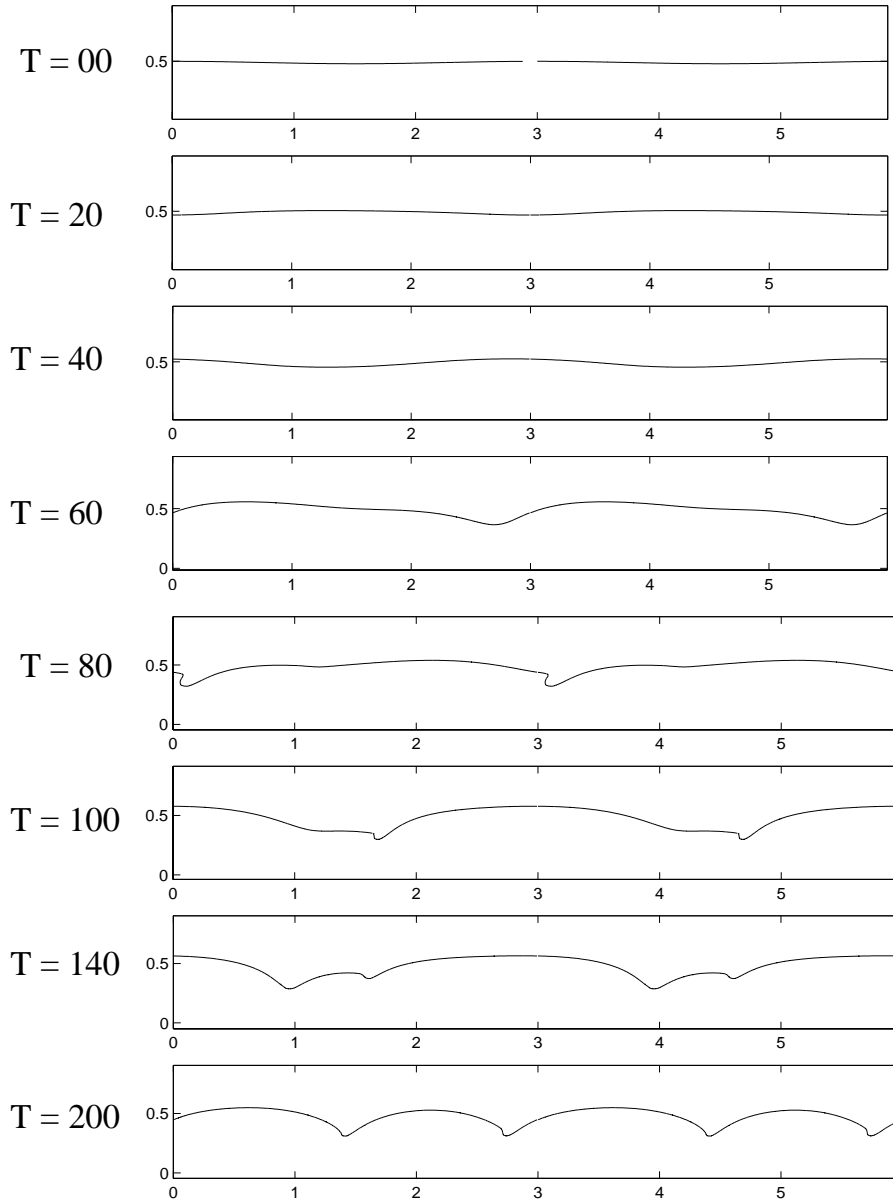


Figure 12: High Reynolds number  $Re = 1149$ .  $m = 0.017$ ,  $l_1 = 0.49$ ,  $T = 0.018$ . Spatial period 3 cm. Temporal evolution of interface shape at times  $t = 0, 20, 40, 60, 80, 100, 140$  and 200.